Theoretical Study of the Benzene Excimer Using Time-Dependent Density Functional Theory

Jay C. Amicangelo*

School of Science, Penn State Erie, The Behrend College, 5091 Stattion Road, Erie, Pennsylvania 16563-0203

Received: June 24, 2005

A theoretical characterization of the potential energy surfaces of the singlet benzene excimer states derived from the B_{2u} monomer excited state has been performed using time-dependent density functional theory. The excited-state potential energy surfaces were initially characterized by computations along the parallel and perpendicular intermolecular translational coordinates. These calculations predict that the lowest excited state for parallel translation is bound with a minimum at 3.15 Å and with a binding energy of 0.46 eV, while the perpendicular translational coordinate was essentially found to be a repulsive state. At the calculated minimum distance, the effect of in-plane rotation, out-of-plane rotation, and slipped-parallel translation were examined. The rotational calculations predict that deviations from the D_{6h} geometry lead to a destabilization of the excimer state; however, small angular variations in the range of 0°−10° are predicted to be energetically feasible. The slipped-parallel translational calculations also predict a destabilizing effect on the excimer state and were found to possess barriers to this type of dissociation in the range of 0.50−0.61 eV. When compared to experimentally determined values for the benzene excimer energetics, the calculated values were found to be in semiquantitative agreement. Overall, this study suggests that the time-dependent density functional theory method can be used to characterize the potential energy surfaces and the energetics of aromatic excimers with reasonable accuracy.

Introduction

An aromatic excimer is a complex between two aromatic molecules that is stable only in the excited state.[1] Pyrene was the first aromatic molecule shown to form excimers in solution, with the key observations being the appearance of a red-shifted, structureless emission band as a function of pyrene concentration, but with no corresponding changes in the absorbance spectrum.[2] Shortly after this initial report, excimer formation was shown to be a photophysical process common to many aromatic molecules.[3−5] A potential energy surface involving the ground state and the lowest excited singlet state of the aromatic molecule as a function of intermonomer separation is generally invoked to explain this phenomenon.[6] The main arguments are as follows. The first step is the excitation of the aromatic monomer to its lowest excited singlet state. This is followed by an attractive collision with a ground-state monomer and the formation of a bound excited-state complex or excimer. Since the interaction is attractive, the energy of the excimer is lower than that of the excited monomer. The intermonomer distance in aromatic excimers is generally thought to be in the range of 3−4 Å, and the energy difference between the excimer and the excited monomer gives the binding energy of the excimer. When the excimer emits a photon to return to the ground state, it is generally believed that the two monomers, at this short distance apart, are in a repulsive portion of the ground-state potential energy curve. As a result, the two ground-state monomers rapidly dissociate before the complex can undergo a single vibrational period.

Several of the experimental parameters that are used to characterize the potential energy surface of aromatic excimers are the transition energy, the binding energy, the ground-state repulsion energy, and the activation energies of association and dissociation, all of which can be determined by spectral measurements.[6−8] Calculational studies of excimers have been performed in an effort to lend theoretical support to the general features of excimer potential energy surfaces and to the experimentally determined excimer parameters.[4,9−15] Much of the theoretical work on excimers to date has been concerned with benzene and naphthalene excimers,[9−12,14,15] since these are the smallest aromatic hydrocarbons for which excimer emission is observed. However, due to the computational cost of excited-state calculations involving aromatic dimers, even for benzene and naphthalene, almost all of the previous theoretical studies have involved approximate or semiempirical methods. In one of the more recent semiempirical studies,[14] the INDO 1/S method[16,17] was used to model the excited-state potential energy surfaces of naphthalene and phenanthrene dimers. It was found, however, that in order to obtain reasonable results for the excimer potential energy surfaces and the excimer energetics, it was necessary to introduce a distance dependence to the $\pi-\sigma$ interaction in one of the resonance integrals. In the one theoretical study in which semiempirical methods were not used,[15] excited-state calculations were performed for naphthalene dimers using the configuration interaction singles (CIS) method with the 6-31G* basis set.[18] However, it was found that several corrective factors, which were basically empirical in nature, had to be applied in order to obtain even qualitatively reasonable results. It has recently been shown that time-dependent density functional theory (TDDFT) is capable of reproducing the singlet excitation energies of conjugated molecules, particularly those of aromatic systems.[19−24] It was the success of the recent TDDFT calculations for the excitation energies of aromatic monomers, combined with the difficulties reported in some of

10.1021/jp053445o CCC: $30.25
Published on Web 09/17/2005

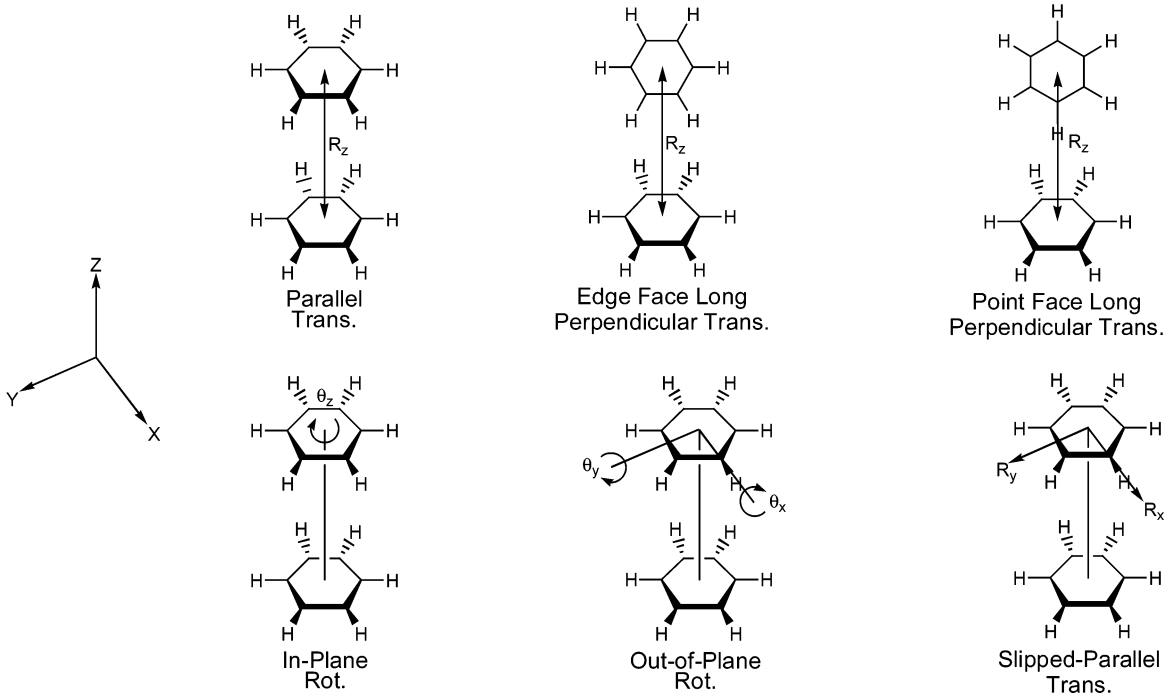

Figure 1. Cartesian coordinate system along with the six basic types of intermolecular coordinates examined for the benzene excimer. The translational coordinates are labeled R_x, R_y, and R_z, and the rotational coordinates are labeled θ_x, θ_y, and θ_z. For each type of motion, only the coordinates varied are displayed. For the in-plane rotation, out-of-plane rotation, and the slipped-parallel translation, the solid line for R_z indicates that this coordinate was held at a fixed value.

the earlier calculations of aromatic excimer potential energy surfaces, that led to the motivation for the current study.

In the present work, the TDDFT method is used to characterize the potential energy surfaces of the singlet benzene excimer states derived from the B_{2u} benzene monomer excited state. The focus of the initial calculations is on the excited-state potential energies for the sandwich dimer and several configurations of the T-shaped dimer as a function of intermonomer distance. These calculations show that the lowest excimer state of the sandwich dimer is bound, while those of the T-shaped dimers are essentially nonbound. Further calculations are then performed, starting with the sandwich dimer at the calculated minimum distance and examining the effect of three other intermolecular coordinates on the excimer-state energies: in-plane rotation, out-of-plane rotation, and slipped-parallel translation. Finally, the calculated energetics of the benzene excimer are compared to available experimentally determined values. Overall, this work demonstrates that the TDDFT method can be used to theoretically characterize the lowest singlet benzene excimer potential energy surface with reasonable accuracy and without the application of empirical correction factors needed in some of the earlier theoretical work on aromatic excimers.

Computational Details

All theoretical calculations were carried out using the Gaussian 98 suite of programs.[25] The B3LYP[26,27] hybrid functional coupled with the 6-31+G* basis set[28,29] was used for all calculations. The B3LYP/6-31+G* level of theory was chosen because this method was shown by Stratman et al.[19] to afford a reasonably good reproduction of the low-lying singlet excited states of the benzene monomer. The ground-state geometry of the benzene monomer was optimized at this level; using the optimized monomer geometry, singlet vertical excitation energies of the benzene dimer (without zero-point energy correction) were calculated using time-dependent density functional theory (TDDFT) as implemented in Gaussian 98.[19] The potential energy surface of the singlet excited states of the benzene dimer derived from the lowest excited state of the benzene monomer (B_{2u} state) was characterized by computations along six basic types of intermolecular coordinates, which are displayed in Figure 1. The translational coordinates are labeled R_x, R_y, and R_z, and the rotational coordinates are labeled θ_x, θ_y, and θ_z.

With the parallel translation of the two benzene monomers along the line defined by the C_6 axis, θ_x, θ_y, and θ_z were set to 0.0°, R_x and R_y were set to 0.0 Å, and R_z was varied from 2.7 to 7.0 Å in increments ranging from 0.05 to 0.4 Å. For the perpendicular translation of the two benzene monomers along the line defined by the C_6 axis, four different configurations were examined. In two of these configurations, designated as edge−face long (EFL) and edge−face short (EFS), θ_x was set to 90.0° and θ_z was set to either 0.0° or 30.0°, respectively. In the other two configurations, designated as point−face short (PFS) and point−face long (PFL), θ_y was set to 90.0° and θ_z was set to either 0.0° or 30.0°, respectively. For simplicity, only the edge−face long and the point−face long configurations are displayed in Figure 1; however, the edge−face short and point−face short configurations are obtained from those given in Figure 1 by a rotation about θ_z by 30°. For all four perpendicular configurations, R_x and R_y were set to 0.0 Å and R_z was varied from 4.0 to 7.0 Å, in increments ranging from 0.1 to 0.25 Å.

For the in-plane rotation of the two benzene monomers about the C_6 axis at a fixed intermonomer distance, θ_x and θ_y were set to 0.0°, R_x and R_y were set to 0.0 Å, R_z was set to 3.15 Å (vide infra), and θ_z was varied from 0.0° to 30.0°, in increments of 2.5°. For the out-of-plane rotation at a fixed intermonomer distance, rotation of the upper monomers about two different axes were investigated: rotation about the axis defined by an opposing pair of C−H bonds, designated as out-of-plane long rotation, and rotation about the axis defined by exactly bisecting two opposing C−C bonds, designated as out-of-plane short rotation. For both out-of-plane rotations, R_x and R_y were set to

0.0 Å and R_z was set to 3.15 Å (vide infra). For the out-of-plane long rotation, θ_y and θ_z were set to 0.0° and θ_x was varied from 0.0° to 30.0°, in increments ranging from 2.5° to 5.0°. For the out-of-plane short rotation, θ_x and θ_z were set to 0.0° and θ_y was varied from 0.0° to 30.0°, in increments ranging from 2.5° to 5.0°.

For the slipped-parallel translation of the two benzene monomers at a fixed intermonomer distance, two coordinates were examined. One was translation along the axis defined by an opposing pair of C−H bonds, designated as slipped-parallel long; the other was translation along the axis defined by bisecting two opposing C−C bonds, designated as slipped-parallel short. For the slipped-parallel long translation, θ_x, θ_y, and θ_z were set to 0.0°, R_y was set to 0.0 Å, R_z was set to 3.15 Å (vide infra), and R_x was varied from 0.0 to 8.0 Å, in increments ranging from 0.2 to 1.0 Å. For the slipped-parallel short translation, θ_x, θ_y, and θ_z were set to 0.0°, R_x was set to 0.0 Å, R_z was set to 3.15 Å (vide infra), and R_y was varied from 0.0 to 8.0 Å, in increments ranging from 0.2 to 1.0 Å.

It is worth noting that this study represents a scan of the excited-state potential energy surfaces along the above-mentioned coordinates and that excited-state geometry optimizations were not performed because geometry optimizations are not implemented in Gaussian 98 in conjunction with time-dependent density functional theory calculations.

Results and Discussion

As mentioned above, the B3LYP/6-31+G* level of theory was chosen because it was shown by Stratman et al.[19] to afford a reasonably good reproduction of the low-lying singlet excited states of the benzene monomer. Calculations employing the BPW91/6-31+G* level of theory, which was also shown to reproduce the monomer transition energies fairly well, were also attempted; however, it was discovered that the calculated excitation energies did not converge to the appropriate monomer values at large intermolecular distances when two monomers were present. Incorrect asymptotic behavior, similar to this, was also observed by Head-Gordon and co-workers when attempting to calculate the energies of charge-transfer excited states for an ethylene−tetrafluoroethylene complex using TDDFT.[30] These authors concluded that the most important effect was the inclusion of a nonlocal Hartree−Fock exchange term, which is present in some hybrid functionals, such as the B3LYP functional. The lack of a nonlocal Hartree−Fock exchange term in the BPW91 hybrid functional is most likely the cause of the failure in the present case.

Monomer Geometry. At the B3LYP/6-31+G* level, the optimized C−C and C−H bond lengths obtained are 1.3988 and 1.0874 Å, respectively. These values can be compared with the recently revised experimental C−C and C−H bond lengths of 1.3914 ± 0.0010 Å and 1.0802 ± 0.0020 Å, respectively, reported by Gauss and Stanton.[31] The calculated bond lengths are slightly larger than the experimental values; however, it is clear from this comparison (relative deviations of 0.5 and 0.7%) that the B3LYP/ 6-31+G* level is in very good agreement with the experimental geometries. Therefore, the use of the B3LYP/ 6-31+G* optimized monomer geometry in the excimer calculations appears justified.

Parallel and Perpendicular Translation Calculations. *Parallel Translation.* The potential energy curves calculated for the parallel translational coordinate of the ground state and the two excimer states derived from the monomer B_{2u} excited-state are displayed in Figure 2. As can be seen from Figure 2, the ground-state potential energy curve is predicted to be repulsive

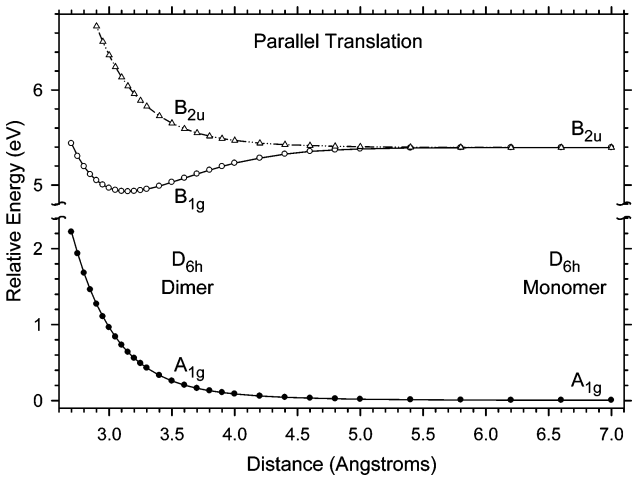

Figure 2. Potential energy curves of the ground state (A_{1g}) of the D_{6h} benzene dimer and the two dimer excited states (B_{1g} and B_{2u}) derived from the B_{2u} monomer excited state as a function of the parallel translation distance. The energies are referenced to the energy of the ground-state monomers at infinite separation.

in this orientation at all distances. It has been shown by several high-level MP2 calculations that benzene dimers in the parallel configuration are, in fact, weakly bound in the ground state.[32,33] It is not unexpected, however, that the current DFT calculations do not predict bound ground-state dimers, as it is known that most DFT methods do not correctly describe the dispersion interactions required to accurately predict ground-state binding energies for weakly bound van der Waals complexes such as the benzene dimer.[34] The excited-state potential energy curves, on the other hand, consist of both a repulsive and an attractive state. In this orientation (D_{6h} symmetry), the B_{2u} state of the isolated monomers is split into a B_{1g} and a B_{2u} excimer state as the distance of the two rings decreases.[35] As is evident from Figure 2, the B_{2u} excimer state is a repulsive state at all distances, while the B_{1g} excimer state is an attractive state possessing an energy minimum at 3.15 Å. The calculated minimum is slightly lower than the value of 3.4−3.5 Å reported in earlier extended Hückel[9] and semiempirical[11] calculations for the parallel benzene excimer. However, it has long been suggested that the distance between rings for aromatic excimers is in the range of 3−4 Å;[3,4] in that regard, the calculated minimum distance is within this range. The behavior of these two states can best be understood by considering the appropriate highest occupied and lowest unoccupied molecular orbitals for the dimer that are involved in the transitions.

The two highest occupied orbitals for the dimer are doubly degenerate e_{1g} and e_{1u} orbitals. The e_{1g} is higher in energy than the e_{1u}, and therefore the e_{1g} is designated the HOMO and the e_{1u} is designated as the HOMO − 1. The two lowest unoccupied dimer orbitals are the doubly degenerate e_{2g} and e_{2u} orbitals. The e_{2g} orbital is lower than the e_{2u} orbital, and therefore the e_{2g} is designated the LUMO and the e_{2u} is designated as the LUMO + 1. The e_{1g} and e_{1u} dimer orbitals are both derived from the monomer e_{1g} orbital, while the e_{2g} and e_{2u} dimer orbitals are both derived from the monomer e_{2u} orbital. In each case, however, the orbitals on the two monomers are oriented differently with respect to one another along the C_6 axis, which allows for different amounts of intermonomer orbital overlap. In the e_{1g} and e_{2u} dimer orbitals, the orbitals on each monomer are oriented in the same direction along the C_6 axis, which allows them to retain their symmetry but does not allow any intermonomer overlap. In the e_{1u} and e_{2g} dimer orbitals, the orbitals on each monomer are oriented in the opposite direction

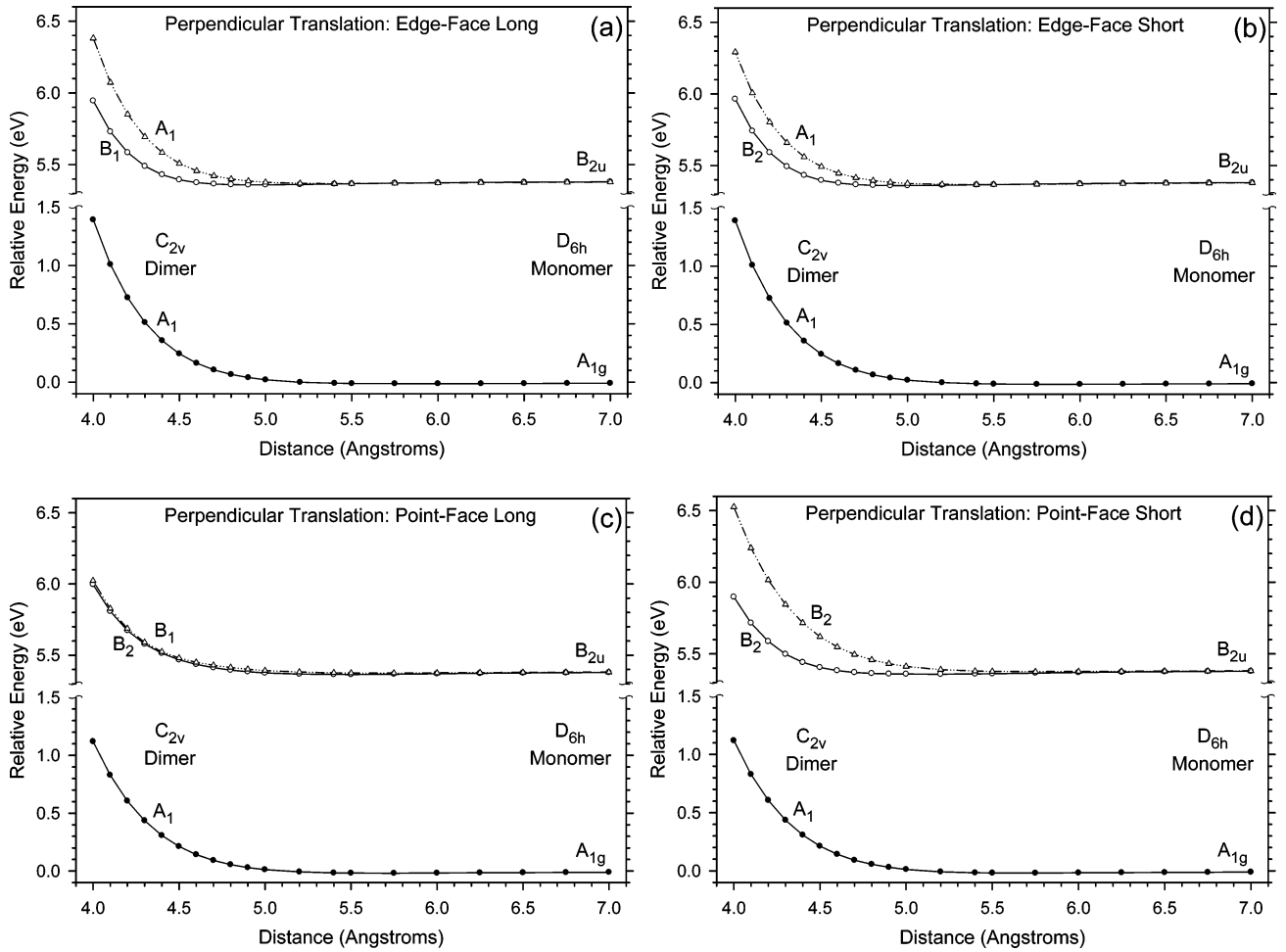

Figure 3. Potential energy curves of the ground state (A_1) of the C_{2v} benzene dimer and the two dimer excited states derived from the B_{2u} monomer excited state as a function of the perpendicular translation distance for the (a) edge−face long, (b) edge−face short, (c) point−face long, and (d) point−face short configurations. The energies are referenced to the energy of the ground-state monomers at infinite separation.

along the C_6 axis, which changes the symmetries of the orbitals and provides for a significant amount of intermonomer overlap. The presence or lack of intermonomer overlap accounts for the energy ordering of these orbitals.

The dominant transition for the B_{1g} state involves the $e_{1g} \rightarrow e_{2g}$ (HOMO → LUMO) orbitals and is characterized by a transfer of an electron from an orbital without positive intermonomer overlap (e_{1g}) to an orbital with considerable intermonomer overlap (e_{2g}). This is why the energy of this state decreases as the translational distance is decreased, in other words, why it is an attractive state. This description is in line with earlier ideas that the attractive nature of the lowest excimer state of aromatic hydrocarbons is due to significant charge-resonance ($M^+M^- \leftrightarrow M^-M^+$) and exciton-resonance ($M^*M \leftrightarrow MM^*$) character,[10,35] which is most efficient when there is considerable intermonomer overlap. The B_{2u} state involves equal contributions of the $e_{1g} \rightarrow e_{2u}$ (HOMO → LUMO + 1) and the $e_{1u} \rightarrow e_{2g}$ (HOMO − 1 → LUMO) orbitals. The $e_{1g} \rightarrow e_{2u}$ transition is characterized by a transfer of an electron between two orbitals without positive intermonomer overlap, and the $e_{1u} \rightarrow e_{2g}$ transition is characterized by a transfer of an electron between two orbitals with positive intermonomer overlap. Overall, this combination appears to cause the energy of this state to increase with decreasing translational distance and thus be a repulsive state.

The energy difference between the B_{2u} state of the isolated monomers and the minimum on the B_{1g} excimer state gives the calculated excimer binding energy in this orientation, which is calculated to be 0.46 eV. This value is higher than the values of 0.19 and 0.17 eV reported in earlier extended Hückel[9] and semiempirical[11] calculations, respectively. The above comparison seems to indicate that inclusion of electron correlation and the less empirical nature of density functional theory have a profound effect on the calculated binding energy for the D_{6h} benzene excimer. The possibility that the TDDFT excimer binding energy was high due to basis-set superposition error (BSSE) was considered; using the counterpoise method,[36,37] the BSSE correction for the ground-state benzene dimer at 3.15 Å was calculated to be 0.03 eV. Assuming that the ground-state correction can be used as an estimate of the excited-state correction, this would only lower the excimer binding energy to 0.43 eV, which is still larger than the results of the earlier calculations. The comparison of the current calculated excimer binding energy to experimentally determined values will not be done here, but rather will be saved until the end of the paper, at which point the excimer energetics as a whole will be discussed.

Perpendicular Translation. The potential energy curves calculated for the four configurations of the perpendicular translational coordinate of the ground state and the two excimer states derived from the monomer B_{2u} excited state are displayed in Figure 3. The point group of each of the perpendicular configurations is C_{2v} and the excited-state symmetry labels shown in Figure 3 correspond to C_{2v} irreducible representations. The ground-state potential energy curves are predicted to be repulsive in all four perpendicular orientations at all distances.

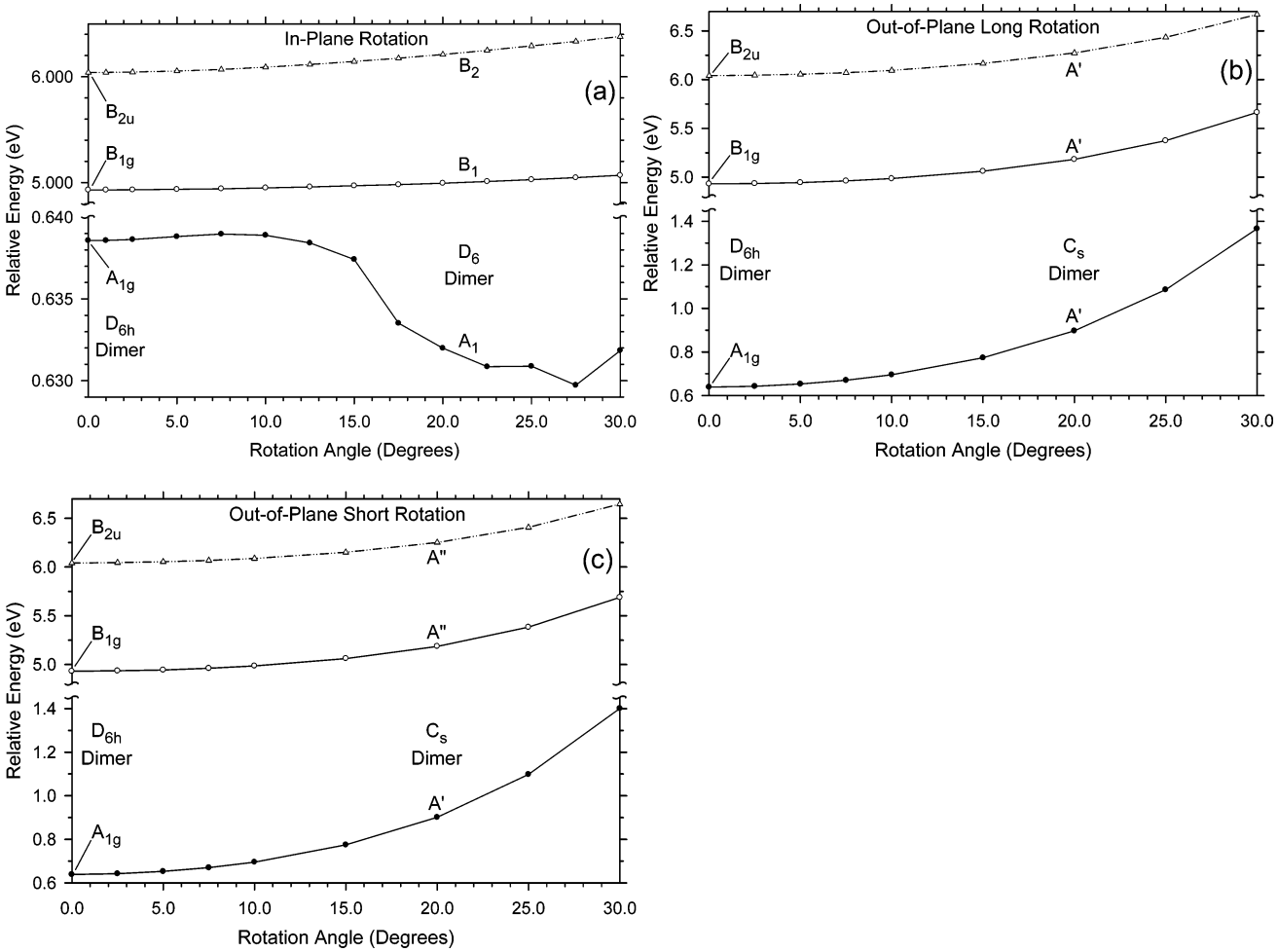

Figure 4. Potential energy curves for the A_{1g} ground state and the B_{1g} and B_{2u} excited states of the D_{6h} benzene dimer at a fixed interplanar distance of 3.15 Å as a function of rotational angle for (a) in-plane rotation, (b) out-of-plane long rotation, and (c) out-of-plane short rotation. For the in-plane rotation (D_6 symmetry), the D_{6h} A_{1g}, B_{1g}, and B_{2u} designations become A_1, B_1, and B_2, respectively. For the out-of-plane rotations (C_s symmetry), the D_{6h} A_{1g}, B_{1g}, and B_{2u} designations become A′, A′, and A′, respectively, for the out-of-plane long rotation and A′, A″, and A″, respectively, for the out-of-plane short rotation. The energies are referenced to the energy of the ground-state monomers at infinite separation.

This is analogous to that observed for the parallel translation. Again, high-level MP2 calculations have shown that the perpendicular benzene dimer is, in fact, bound in the ground state,[32,33] and the deficiency in the current DFT calculations is due to the incorrect description of the necessary dispersion interactions.[34] For all four of the perpendicular configurations, both excited-state potential energy curves appear to be repulsive in nature. On closer inspection, however, the lower of the two excited states is actually predicted to be very weakly bound with very shallow minima at 4.9, 4.9, 5.2, and 5.5 Å for the EFL, EFS, PFL, and PFS configurations, respectively. The binding energies, calculated as the difference between the B_{2u} monomer energy and the energy at the minimum, are predicted to be 0.02 eV for the EFL and PFL configurations and 0.03 eV for the EFS and PFS configurations. Comparing these small binding energies for the perpendicular orientations to the 0.46 eV binding energy of the parallel orientation, it is clear that the parallel (D_{6h}) conformation is the more energetically favorable geometry for the benzene excimer. This understandable considering that, as described above, the attractive nature of the lowest excimer state for the D_{6h} excimer is primarily due to the transfer of an electron from an orbital without positive intermonomer overlap to an orbital with considerable intermonomer overlap. In the perpendicular configurations, this type of intermonomer overlap in considerably reduced for the highest occupied and lowest unoccupied orbitals, and therefore the attractive nature of these states is also substantially reduced. For all practical purposes, with such small binding energies, the TDDFT calculations predict that the lowest excited states of the perpendicular configurations are all essentially unbound.

Rotation and Slipped-Parallel Translation Calculations. On the basis of the results that the parallel configuration is predicted to be significantly more stable than any of the perpendicular configurations, further calculations were performed starting from the parallel orientation at the calculated minimum distance to assess the effect of in-plane and out-of-plane rotation and slipped-parallel translation on the B_{1g} and B_{2u} excited-state energies. In all of the calculations described below, the intermonomer distance was fixed at 3.15 Å, and the two rings were either rotated or translated with respect to one another.

In-Plane Rotation. The potential energy curves calculated for the ground state and the B_{1g} and B_{2u} excimer states as a function of the in-plane rotational coordinate are displayed in Figure 4a. As the two parallel benzene rings are rotated, the symmetry of the dimer is reduced from D_{6h} to D_6. With this lowering of the symmetry, the B_{1g} and B_{2u} symmetry labels of the excited states for the D_{6h} excimer become B_1 and B_2 symmetry labels within the D_6 point group, as is expected from group theory correlation tables.[38] The ground-state potential energy curve is predicted to stay approximately level as the two benzene rings are rotated from 0° to 10°. After 10°, the energy decreases by approximately

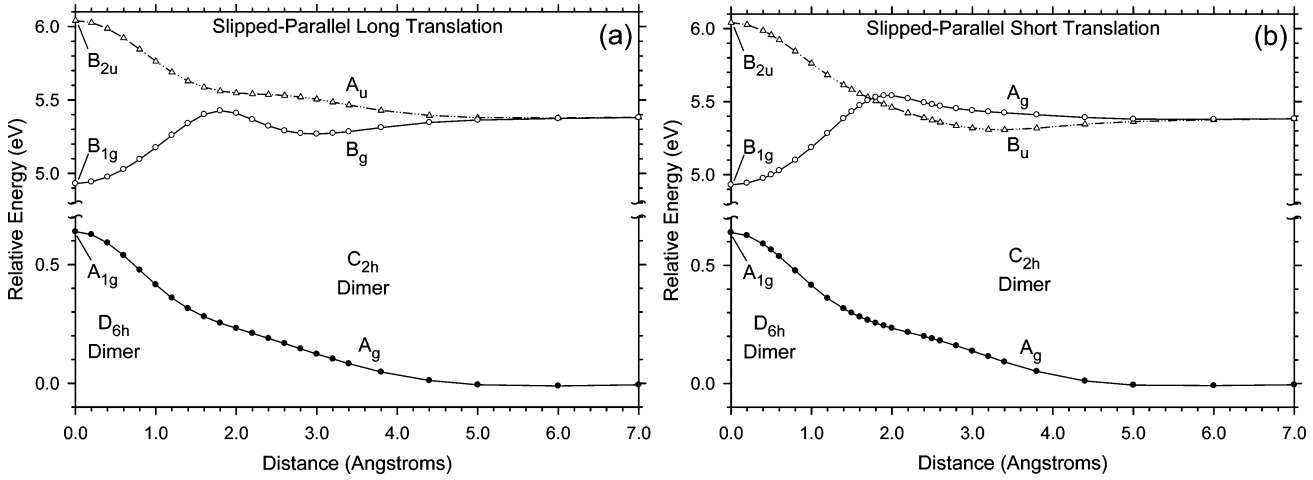

Figure 5. Potential energy curves for the A_{1g} ground state and the B_{1g} and B_{2u} excited states of the D_{6h} benzene dimer at a fixed interplanar distance of 3.15 Å as a function of slipped-parallel translation distance for (a) slipped-parallel long translation and (b) slipped-parallel short translation. For slipped-parallel translation (C_{2h} symmetry), the D_{6h} A_{1g}, B_{1g}, and B_{2u} designations become A_g, B_g, and A_u, respectively, for the slipped-parallel long translation and A_g, B_u, and A_g, respectively, for the slipped-parallel short translation. The energies are referenced to the energy of the ground-state monomers at infinite separation.

0.01 eV, as the steric repulsions between the atoms on each ring are reduced. The B_{1g} and B_{2u} excited-state energies are both predicted to increase with in-plane rotation, although the rate of increase and the overall energy change for the B_{2u} state is clearly larger than that for the B_{1g} state. The overall changes in energy for the B_{1g} and B_{2g} states from 0° to 30° are calculated to be 0.14 and 0.34 eV, respectively. These results show that, in general, in-plane rotation of the two benzene rings destabilizes the D_{6h} excimer states, and therefore the D_{6h} excimer geometry is more stable. A closer examination of the energy change for the B_{1g} state, however, reveals that a significant change in energy does not occur until approximately after 10°, with the change in energy from 0° to 10° being 0.02 eV. This suggests that there might be a small amount of fluxional behavior in terms of in-plane rotation for the lowest benzene excimer state, but clearly not free rotation. The current results are in general agreement with earlier extended Hückel[9] and semiempirical calculations,[11] in that these also predicted that in-plane rotation destabilizes the D_{6h} excimer. However, both calculations predicted "barriers" of 0.01 eV, which is much lower than the current calculations. Therefore, the earlier calculations predicted essentially free in-plane rotation of the two benzene rings for the excimer.

Out-of-Plane Rotation. The potential energy curves calculated for the ground state and the B_{1g} and B_{2u} excimer states as a function of the out-of-plane long and out-of-plane short rotational coordinates are displayed in Figure 4, parts b and c, respectively. As the two parallel benzene rings are rotated out-of-plane, the symmetry of the dimer is reduced from D_{6h} to C_s. With this lowering of the symmetry, the B_{1g} and B_{2u} symmetry labels of the excited states for the D_{6h} excimer become A′ symmetry labels for the out-of-plane long rotation and A″ symmetry labels for the out-of-plane short rotation, as is expected from group theory correlation tables.[38] The ground-state potential energy curves are predicted to increase upon out-of-plane rotation for both the long and short rotations. The increase in energy for both types of rotation is small (0.01 eV) until 5°, and then it increases more rapidly for angles greater than 5°. The overall change in energy from 0° to 30° is 0.73 and 0.76 eV for the out-of-plane long and short rotation, respectively. Although, calculations were not performed for out-of-plane angles larger than 30.0°, presumably the energy of the ground state would continue to rise until reaching a maximum at 90.0°. The B_{1g} and B_{2u} D_{6h} excited-state energies are both predicted to increase with out-of-plane rotation. The rate of increase in energy for both states appears to be very similar, although the B_{1g} state increases slightly more rapidly than the B_{2u} state. The overall energy changes for the B_{1g} and B_{2u} states from 0° to 30° are calculated to be 0.73 and 0.63 eV, respectively, for the out-of-plane long rotation and 0.76 and 0.60 eV, respectively, for the out-of-plane short rotation. Although, calculations were not performed for angles larger than 30.0°, presumably the energy of the excited states would continue to rise until reaching a maximum at 90.0°. Comparing the energy changes for the two out-of-plane rotations, it is clear that both types of rotation destabilize the D_{6h} excimer states to an approximately equal degree. Similar to the in-plane rotation, an examination of the energy change for the B_{1g} state at small angles reveals small energy changes (0.01 eV) between 0° and 5° rotations. This again suggests a small amount of fluxional behavior in terms of out-of-plane rotation for the lowest benzene excimer state. The current results are in disagreement with earlier semiempirical calculations,[11] in that the semiempirical calculations predict that an out-of-plane rotation of 5° actually stabilizes the lowest-energy excimer state by approximately 0.03 eV for both types of rotation. At angles greater than 5°, these calculations predicted a steep increase in the energy of the lowest excimer state. It is unclear why the earlier calculations predicted a stabilization of the energy of the lowest excimer state with out-of-plane rotation, given that this type of motion will most certainly decrease the amount of intermonomer overlap.

Slipped-Parallel Translation. The potential energy curves calculated for the ground state and the B_{1g} and B_{2u} excimer states as a function of the slipped-parallel long and short translational coordinates are displayed in Figure 5. As the two parallel benzene rings are translated in this manner, the symmetry of the dimer is reduced from D_{6h} to C_{2h}. With this lowering of the symmetry, the B_{1g} and B_{2u} excited-state symmetry labels of the D_{6h} excimer become B_g and A_u symmetry labels, respectively, for the slipped-parallel long translation and A_g and B_u symmetry labels, respectively, for the slipped-parallel short translation, as is expected from group theory correlation tables.[38] The ground-state potential energy curves for both types of translation are quite similar to one another and are predicted to decrease upon slipped-parallel translation. The initial decrease is quite rapid until approximately 1.4 Å for the slipped-parallel long and 1.2 Å for the slipped-

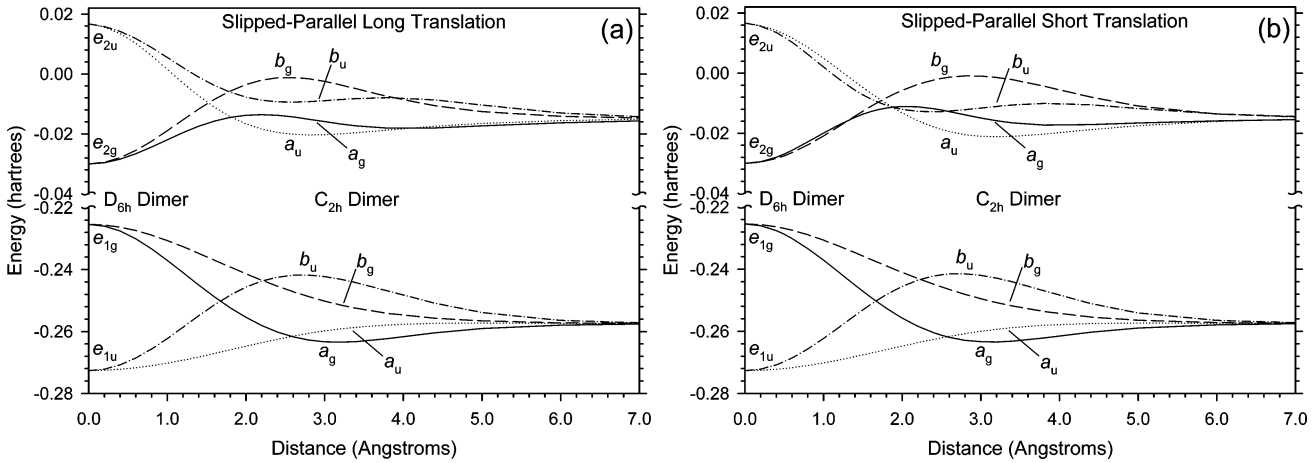

Figure 6. Energies of the occupied e_{1g} and e_{1u} orbitals and the unoccupied e_{2g} and e_{2u} orbitals for the D_{6h} benzene dimer at a fixed interplanar distance of 3.15 Å as a function of slipped-parallel translation distance for (a) slipped-parallel long translation and (b) slipped-parallel short translation. For slipped-parallel translation (C_{2h} symmetry), the D_{6h} e_{1g} and e_{2g} orbitals are each split into a_g and b_g orbitals and the e_{1u} and e_{2u} orbitals are each split into a_u and b_u orbitals.

parallel short, at which point the rate of decrease slows down until the energy converges to the isolated monomer energies at approximately 6 Å. The distances at which the rate of decrease changes correspond to the point at which the rings are displaced approximately halfway with respect to one another. The behavior of the B_{1g} and B_{2u} excited states, on the other hand, is quite different for the two types of slipped-parallel translation. For the slipped-parallel long translation, Figure 5a, the energy of the B_{1g} state (B_g in C_{2h}) is initially predicted to rapidly increase, reaching a maximum (0.50 eV calculated from 0.0 Å) at 1.8 Å. The energy of this state is then predicted to decrease into a shallow minimum (0.12 eV calculated from the B_{2u} monomer state) at approximately 3.0 Å, followed by a slow increase, and finally a convergence to the monomer B_{2u} state energy. The energy of the dimer B_{2u} state (A_u in C_{2h}) for this type of translation is predicted to rapidly decrease until 1.8 Å, at which point the rate of change slows down until the energy of this state eventually converges to the energy of the B_{2u} monomer state. For the slipped-parallel short translation, Figure 5b, the energy of the B_{1g} state (A_g in C_{2h}) is also predicted to initially increase and reaches a maximum (0.61 eV calculated from 0.0 Å) at approximately 1.9−2.0 Å. This is then followed by a slow decrease to the monomer B_{2u} state energy, without passing through a minimum. The dimer B_{2u} state (B_u in C_{2h}) for this type of translation rapidly decreases, and at 1.8 Å the energy of this state becomes lower than that of the B_{1g} (A_g in C_{2h}) state. Past 1.8 Å, the energy of this state continues to decrease, reaching a minimum (0.08 eV calculated from the B_{2u} monomer state) at approximately 3.4 Å, followed by a slow convergence to the energy of the B_{2u} monomer state.

The behavior of each of these states for the two types of translation can best be understood by considering the variation of the energies of the appropriate highest occupied and lowest unoccupied molecular orbitals as a function of translational distance, which is shown in Figure 6. As described above, in the D_{6h} configuration, the highest occupied orbitals consist of an e_{1g} and e_{1u} set, and the lowest unoccupied orbitals consist of an e_{2g} and e_{2u} set. The dominant transition for the B_{1g} state involves the $e_{1g} \rightarrow e_{2g}$ (HOMO → LUMO) orbitals. The dominant transition for the B_{2u} state involves equal contributions of the $e_{1g} \rightarrow e_{2u}$ (HOMO → LUMO + 1) and the $e_{1u} \rightarrow e_{2g}$ (HOMO − 1 → LUMO) orbitals; however, for the current discussion, only the $e_{1g} \rightarrow e_{2u}$ (HOMO → LUMO + 1) orbital transition is important. When the two rings are translated with respect to one another, the symmetry and the degeneracy of these orbitals is lifted, with the e_{1g} and e_{2g} orbitals becoming a_g and b_g orbitals and the e_{1u} and e_{2u} orbitals becoming a_u and b_u orbitals. As can be seen from Figure 6, the energies of these orbitals vary considerably as a function of the translational distance, with several orbitals crossing one another. It is the shapes of the orbital energy variations and the crossings that give rise to the calculated behaviors of the B_{1g} and B_{2u} excited states for the two types of slipped-parallel translation.

For the slipped-parallel long translation, the B_{1g} state becomes a B_g state in C_{2h} symmetry, and from 0 to 1.8 Å the dominant orbital transition involves the $b_g \rightarrow a_g$ orbitals. At 1.8 Å the upper a_u orbital crosses the a_g orbital, and after this distance the dominant transition involves the $b_u \rightarrow a_u$ orbitals. It is the crossing of these orbitals and the decreasing versus increasing characteristic of the orbital energy variations that give rise to the maximum and the minimum in the B_{1g} (B_g in C_{2h}) potential energy curve. The B_{2u} state in this orientation becomes an A_u state in C_{2h} symmetry, and over the range of distances examined the dominant orbital transition for this state involves the $b_g \rightarrow b_u$ orbitals. In this case, it is the energy variation of the b_u orbital that results in the calculated behavior of the B_{2u} (A_u in C_{2h}) state with translational distance.

For the slipped-parallel short translation, the B_{1g} state becomes an A_g state in C_{2h} symmetry, and from 0 to 1.7 Å the dominant orbital transition involves the $b_g \rightarrow b_g$ orbitals. Between 1.7 and 2.0 Å, the $b_u \rightarrow b_u$ configuration becomes more prominent in the transition; by 2.0 Å, it has become the dominant configuration. Similar to the slipped-parallel long translation, the orbital crossings and the shapes of the energy variations cause the B_{1g} (A_g in C_{2h}) state energy to reach a maximum and then begin to decrease. However, in this case, the decrease in the energy of the b_u orbital is not large enough for this state to reach a minimum. The B_{2u} state in this orientation becomes a B_u state in C_{2h} symmetry; over the range of distances examined, the dominant orbital transition for this state involves the $b_g \rightarrow a_u$ orbitals, although the $b_u \rightarrow a_g$ configuration begins to become prominent after 2.0 Å. Overall, however, it appears that the energy variation of the upper a_u orbital and the crossing of the upper a_u and b_u orbitals is what causes the energy of the B_{2u} (B_u in C_{2h}) state to become lower than that of the B_{1g} (A_g in C_{2h}) state beyond 1.8 Å.

Excimer Energetics. From the above discussion, it is clear that the present TDDFT excited-state calculations predict the

TABLE 1: Binding Energies, Transition Energies, Ground-State Repulsion Energies, and Activation Energies (in eV) for the Benzene Excimer

parameter	theory	experiment
binding energy	0.46	0.22,[a] 0.36,[b] 0.35[c]
transition energy	4.29	3.88,[a] 3.92,[b] 3.91[c]
repulsion energy	0.63	0.48,[a] 0.42,[b] 0.46[c]
dissociation activation energy	0.50,[d] 0.61[e]	0.37,[b] 0.368[f]
association activation energy	0.12,[d] 0.08[e]	0.10,[b] 0.113[f]

[a] Ref 8. [b] Ref 39. [c] Ref 40. [d] Calculated from slipped-parallel long translation. [e] Calculated from slipped-parallel short translation. [f] Ref 41.

parallel, D_{6h} orientation to be the most energetically stable geometry for the benzene excimer. At the minimum distance of 3.15 Å, various energetic parameters of the excimer, such as binding energy, transition energy, and ground-state repulsion energy, can be calculated and compared to experimental literature values.[8,39−41] These quantities are presented in Table 1.

As can be seen from Table 1, the calculated values of binding energy, transition energy, and repulsion energy are all higher than the experimental literature values. The deviations between the calculated and experimental values of the binding energy are 0.24 eV for the first value listed and 0.10 and 0.11 eV for the latter two values. However, as discussed by Cundall and Robinson,[40,42] the binding energy determined by Birks and coworkers (0.22 eV)[8] should be considered a lower limit because these authors neglected to consider the temperature dependence of the rate constant for excimer fluorescence, which does affect the determination of the excimer binding energy. With that factor in mind, the agreement between the theoretical value and the remaining two experimental literature values is quite reasonable. The deviations between the calculated and experimental transition energies are found to be 0.41, 0.37, and 0.38 eV. Given that the deviation between the calculated and experimental B_{2u} transition energy for the benzene monomer is 0.50 eV,[19] the level of disagreement found for the excimer transition energy seems acceptable. The deviations between the calculated and experimental ground-state repulsion energies are 0.15, 0.21, and 0.17 eV, which also seem reasonable since the experimental values of the repulsion energy are the least accurately known of the above excimer parameters. These results suggest that the TDDFT method using the B3LYP hybrid functional can be used to give a semiquantitative characterization of these primary energetic parameters of the benzene excimer. Further work is in progress to determine if this method can correctly predict experimental trends in these parameters for other aromatic excimers.

Values of the excimer dissociation and association activation energies have been experimentally determined to be approximately 0.37 and 0.1 eV, respectively (see Table 1). The D_{6h}, parallel translation does not predict an activation energy for excimer dissociation or association, and so this coordinate cannot be used to estimate these values. Considering the magnitudes of the experimentally determined activation energies, it seems plausible that the barriers calculated from the slipped-parallel translational motion might be a good model for theoretically assessing these parameters. The energy barriers calculated for the long and short slipped-parallel dissociation relative to the D_{6h} dimer energy are calculated to be 0.50 and 0.61 eV, respectively, and the association barriers for the long and short slipped-parallel translation relative to the B_{2u} monomer energy are calculated to be 0.12 and 0.08 eV, respectively. The deviations between the experimental dissociation activation energies and the calculated values are essentially 0.13 and 0.24 eV for the slipped-parallel long and short translation, respectively, while the deviations between the experimental association activation energies and the calculated values range from 0.007 to 0.033 eV. Considering the magnitudes of the deviations for the binding, transition, and ground-state repulsion energies, these deviations are reasonable and suggest that the barriers calculated from slipped-parallel translation may provide semiquantitative predictions of excimer activation energies. However, further studies would be required to assess whether excimer activation energy trends among other aromatic molecules can be successfully predicted using this method.

Conclusion

A theoretical characterization of the potential energy surfaces of the singlet benzene excimer states derived from the B_{2u} monomer excited state has been performed with time-dependent density functional theory using the B3LYP hybrid functional and the 6-31+G* basis set. The potential energy surface of the lowest singlet excimer state was initially characterized by computations along two basic intermolecular coordinates: parallel (D_{6h}) and perpendicular (C_{2v}) translation of two benzene monomers along the centroid axes. These calculations predicted that the lowest excited state for parallel translation is a bound state with a binding energy of 0.46 eV and that the lowest excited state for perpendicular translation was essentially a nonbound or repulsive state. At the calculated minimum distance for the parallel excimer, the effect of in-plane and out-of-plane rotation of the two monomers and slipped-parallel translation of the two monomers along the long and short monomer axes were examined. The rotational calculations predict that deviations from the D_{6h} geometry lead to an overall destabilization of the lowest excimer state; however, small angular variations in the range of 0°−10° are predicted to be energetically feasible. The slipped-parallel translation calculations also predict a destabilizing effect on the lowest excimer state, and barriers to this type of dissociation were found to be in the range of 0.50−0.61 eV. When compared to experimentally determined values for the excimer energetics, the calculated values were found to be in reasonable semiquantitative agreement. Overall, this study suggests that the TDDFT method can be used to characterize the potential energy surfaces and energetics of aromatic excimers with reasonable accuracy.

Acknowledgment. This work was supported by startup funds from Penn State Erie, The Behrend College. I thank Jessica Collier for help with extracting state energies and state symmetries from the Gaussian output files for some of the calculations.

Supporting Information Available: A text (.txt) file containing sample Gaussian 98 input files for all of the types of calculations performed in this work. This material is available free of charge via the Internet at http://pubs.acs.org.

References and Notes

(1) Stevens, B.; Hutton, E. *Nature* **1960**, *186*, 1045.
(2) Forster, T.; Kasper, K. *Z. Phys. Chem. N. F.* **1954**, *1*, 275.
(3) Birks, J. B. *Acta Phys. Polon.* **1964**, *26*, 367.
(4) Birks, J. B. *Prog. React. Kinet.* **1970**, *5*, 181.
(5) Birks, J. B. In *Photophysics of Aromatic Molecules*; Wiley-Interscience: London, 1970; pp 301−371.
(6) Stevens, B.; Ban, M. I. *Trans. Faraday Soc.* **1964**, *60*, 1515.
(7) Birks, J. B.; Lumb, M. D.; Munro, I. H. *Proc. R. Soc. (London) A* **1964**, *280*, 289.

(8) Birks, J. B.; Braga, C. L.; Lumb, M. D. *Proc. R. Soc. (London) A* **1965**, *283*, 83.
(9) Chesnut, D. B.; Fritchie, C. J.; Simmons, H. E. *J. Chem. Phys.* **1965**, *42*, 1127.
(10) Vala, M. T.; Hillier, I. H.; Rice, S. A.; Jortner, J. *J. Chem. Phys.* **1966**, *44*, 23.
(11) Srinivasan, B. N.; Russell, J. V.; McGlynn, S. P. *J. Chem. Phys.* **1968**, *48*, 1931.
(12) Chandra, A. K.; Lim, E. C. *J. Chem. Phys.* **1968**, *48*, 2589.
(13) Minn, F. L.; Pinion, J. P.; Filipescu, N. *J. Phys. Chem.* **1971**, *75*, 1794.
(14) Sadygov, R. G.; Lim, E. C. *Chem. Phys. Lett.* **1994**, *225*, 441.
(15) East, A. L. L.; Lim, E. C. *J. Chem. Phys.* **2000**, *113*, 8981.
(16) Ridley, J.; Zerner, M. *Theor. Chim. Acta* **1973**, *32*, 111.
(17) Ridley, J. E.; Zerner, M. C. *Theor. Chim. Acta* **1976**, *42*, 223.
(18) Foresman, J. B.; Head-Gordon, M.; Polpe, J. A.; Frisch, M. J. *J. Phys. Chem.* **1992**, *96*, 135.
(19) Stratmann, R. E.; Scuseria, G. E.; Frisch, M. J. *J. Chem. Phys.* **1998**, *106*, 8218.
(20) Adamo, C.; Scuseria, G. E.; Barone, V. *J. Chem. Phys.* **1999**, *111*, 2889.
(21) Hirata, S.; Head-Gordon, M.; Bartlett, R. J. *J. Chem. Phys.* **1999**, *111*, 10774.
(22) Heinze, H. H.; Gorling, A.; Rosch, N. *J. Chem. Phys.* **2000**, *113*, 2088.
(23) Hsu, C.-P.; Hirata, S.; Head-Gordon, M. *J. Phys. Chem. A* **2001**, *105*, 451.
(24) Halasinski, T. M.; Weisman, J. L.; Ruiterkamp, R.; Lee, T. J.; Salama, F.; Head-Gordon, M. *J. Phys. Chem. A* **2003**, *107*, 3660.
(25) Frisch, M. J.; Trucks, G. W.; Schlegel, H. B.; Scuseria, G. E.; Robb, M. A.; Cheeseman, J. R.; Zakrzewski, V. G.; Montgomery, J. A., Jr.; Stratmann, R. E.; Burant, J. C.; Dapprich, S.; Millam, J. M.; Daniels, A. D.; Kundin, K. N.; Strain, M. C.; Farkas, O.; Tomasi, J.; Barone, V.; Cossi, M.; Cammi, R.; Mennucci, B.; Pomelli, C.; Adamo, C.; Clifford, S.; Ochterski, J.; Petersson, G. A.; Ayala, P. Y.; Cui, Q.; Morokuma, K.; Malick, D. K.; Rabuck, A. D.; Raghavachari, K.; Foresman, J. B.; Cioslowski, J.; Ortiz, J. V.; Stefanov, B. B.; Liu, G.; Liashenko, A.; Piskorz, P.; Komaromi, I.; Gomperts, R.; Martin, R. L.; Fox, D. J.; Keith, T.; Al-Laham, M. A.; Peng, C. Y.; Nanayakkara, A.; Gonzalez, C.; Challacombe, M.; Gill, P. M. W.; Johnson, B.; Chen, W.; Wong, M. W.; Andres, J. L.; Gonzalez, C.; Head-Gordon, M.; Replogle, E. S.; Pople, J. A. *Gaussian 98*, Revision A.11; Gaussian, Inc.: Pittsburgh, PA, 1998.
(26) Becke, A. D. *J. Chem. Phys.* **1993**, *98*, 5648.
(27) Lee, C.; Yang, W.; Parr, R. G. *Phys. Rev. B* **1988**, *37*, 785.
(28) Frisch, M. J.; Pople, J. A.; Binkley, J. S. *J. Chem. Phys.* **1984**, *80*, 3265.
(29) Clark, T.; Chandrasekhar, J.; Spitznagel, G. W.; Schleyer, P. V. R. *J. Comput. Chem.* **1983**, *4*, 294.
(30) Dreuw, A.; Weisman, J. L.; Head-Gordon, M. *J. Chem. Phys.* **2003**, *119*, 2943.
(31) Gauss, J.; Stanton, J. F. *J. Phys. Chem. A* **2000**, *104*, 2865.
(32) Sinnokrot, M. O.; Valeev, E. F.; Sherrill, C. D. *J. Am. Chem. Soc.* **2002**, *124*, 10887.
(33) Sinnokrot, M. O.; Sherrill, C. D. *J. Phys. Chem. A* **2004**, *108*, 10200.
(34) Tsuzuki, S.; Luthi, H. P. *J. Chem. Phys.* **2001**, *114*, 3949.
(35) Azumi, T.; McGlynn, S. P. *J. Chem. Phys.* **1965**, *42*, 1675.
(36) Boys, S. F.; Bernardi, R. *Mol. Phys.* **1970**, *19*, 553.
(37) van Duijneveldt, F. B.; van Duijneveldt-van de Rijdt, J. G. C. M.; van Lenthe, J. H. *Chem. Rev.* **1994**, *94*, 1873.
(38) Wilson, E. B.; Decius, J. C.; Cross, P. C. *Molecular Vibrations: The Theory of Infrared and Raman Vibrational Spectra*; McGraw-Hill: New York, 1955.
(39) Hirayama, F.; Lipsky, S. *J. Chem. Phys.* **1969**, *51*, 1939.
(40) Cundall, R. B.; Robinson, D. A. *J. Chem. Soc., Faraday Trans. 2* **1972**, *68*, 1133.
(41) Gregory, T. A.; Helman, W. P. *J. Chem. Phys.* **1972**, *56*, 377.
(42) Cundall, R. B.; Robinson, D. A. *Chem. Phys. Lett.* **1972**, *13*, 257.